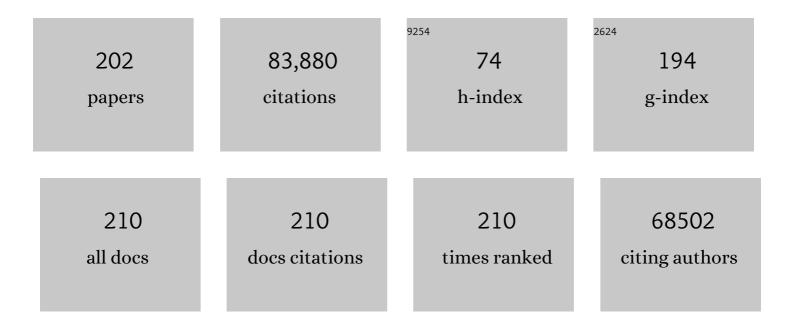
## Yuegang Zhang

List of Publications by Year in descending order

Source: https://exaly.com/author-pdf/7345731/publications.pdf Version: 2024-02-01



#	Article	IF	CITATIONS
1	Tailoring Mg <sup>2+</sup> Solvation Structure in a Facile Allâ€Inorganic [Mg <sub>x</sub> Li <sub>y</sub> Cl <sub>2x+y</sub> · <i>n</i> THF] Complex Electrolyte for High Rate and Long Cycleâ€Life Mg Battery. Energy and Environmental Materials, 2023, 6, .	7.3	13
2	Construction of Moisture‣table Lithium Diffusionâ€Controlling Layer toward High Performance Dendriteâ€Free Lithium Anode. Advanced Functional Materials, 2022, 32, 2110468.	7.8	32
3	Effect of Mg Cation Diffusion Coefficient on Mg Dendrite Formation. ACS Applied Materials & Interfaces, 2022, 14, 6499-6506.	4.0	14
4	A flexible artificial solid-electrolyte interlayer supported by compactness-tailored carbon nanotube network for dendrite-free lithium metal anode. Journal of Energy Chemistry, 2022, 69, 421-427.	7.1	8
5	A facile in situ Mg surface chemistry strategy for conditioning-free Mg[AlCl4]2 electrolytes. Electrochimica Acta, 2022, 414, 140213.	2.6	6
6	Stable Solid Electrolyte Interphase In Situ Formed on Magnesiumâ€Metal Anode by using a Perfluorinated Alkoxideâ€Based Allâ€Magnesium Salt Electrolyte. Advanced Materials, 2022, 34, .	11.1	41
7	Simultaneous optimization of solvation structure and water-resistant capability of MgCl2-based electrolyte using an additive combination of organic and inorganic lithium salts. Energy Storage Materials, 2022, 51, 873-881.	9.5	12
8	Unraveling Shuttle Effect and Suppression Strategy in Lithium/Sulfur Cells by In Situ/Operando Xâ€ray Absorption Spectroscopic Characterization. Energy and Environmental Materials, 2021, 4, 222-228.	7.3	31
9	In Situ Selfâ€Assembly of Ordered Organic/Inorganic Dualâ€Layered Interphase for Achieving Longâ€Life Dendriteâ€Free Li Metal Anodes in LiFSIâ€Based Electrolyte. Advanced Functional Materials, 2021, 31, 2007434.	7.8	65
10	Strong adsorption, catalysis and lithiophilic modulation of carbon nitride for lithium/sulfur battery. Nanotechnology, 2021, 32, 192002.	1.3	7
11	Infrared study of the multiband low-energy excitations of the topological antiferromagnet <mml:math xmlns:mml="http://www.w3.org/1998/Math/MathML"&gt;<mml:mrow><mml:msub><mml:mi>MnBi</mml:mi><mr Physical Review B, 2021, 103, .</mr </mml:msub></mml:mrow></mml:math 	nl:mn>2 </td <td>13 mmi:mn&gt;</td>	13 mmi:mn>
12	Unzipped Carbon Nanotube/Graphene Hybrid Fiber with Less "Dead Volume―for Ultrahigh Volumetric Energy Density Supercapacitors. Advanced Functional Materials, 2021, 31, 2100195.	7.8	76
13	Mechanistic Investigation of Polymerâ€Based Allâ€Solidâ€State Lithium/Sulfur Battery. Advanced Functional Materials, 2021, 31, 2104863.	7.8	26
14	Reconfigurable Tunneling Transistors Heterostructured by an Individual Carbon Nanotube and MoS <sub>2</sub> . Nano Letters, 2021, 21, 6843-6850.	4.5	11
15	Reversible function switching of Ag catalyst in Mg/S battery with chloride-containing electrolyte. Energy Storage Materials, 2021, 42, 513-516.	9.5	9
16	ldentifying Water Oxidation Mechanisms at Pure and Titaniumâ€Doped Hematiteâ€Based Photoanodes with Spectroelectrochemistry. Small Methods, 2021, 5, e2100976.	4.6	10
17	In-situ growth of vertically aligned nickel cobalt sulfide nanowires on carbon nanotube fibers for high capacitance all-solid-state asymmetric fiber-supercapacitors. Journal of Energy Chemistry, 2020, 41, 209-215.	7.1	75
18	Antiferromagnetic topological insulator MnBi <sub>2</sub> Te <sub>4</sub> : synthesis and magnetic properties. Physical Chemistry Chemical Physics, 2020, 22, 556-563.	1.3	88

#	Article	IF	CITATIONS
19	High energy density lithium metal batteries enabled by a porous graphene/MgF2 framework. Energy Storage Materials, 2020, 26, 73-82.	9.5	79
20	Boosting electrocatalytic oxygen evolution using ultrathin carbon protected iron–cobalt carbonate hydroxide nanoneedle arrays. Journal of Power Sources, 2020, 450, 227639.	4.0	23
21	Extending Cycle Life of Mg/S Battery by Activation of Mg Anode/Electrolyte Interface through an LiClâ€Assisted MgCl <sub>2</sub> Solubilization Mechanism. Advanced Functional Materials, 2020, 30, 1909370.	7.8	49
22	Scalable microgel spinning of a three-dimensional porous graphene fiber for high-performance flexible supercapacitors. Journal of Materials Chemistry A, 2020, 8, 25355-25362.	5.2	41
23	Flexible Electrocatalytic Nanofiber Membrane Reactor for Lithium/Sulfur Conversion Chemistry. Advanced Functional Materials, 2020, 30, 1910533.	7.8	41
24	A stretchable, asymmetric, coaxial fiber-shaped supercapacitor for wearable electronics. Nano Research, 2020, 13, 1686-1692.	5.8	46
25	Asymmetric gel polymer electrolyte with high lithium ion conductivity for dendrite-free lithium metal batteries. Journal of Materials Chemistry A, 2020, 8, 8033-8040.	5.2	93
26	Recent advances in research on anodes for safe and efficient lithium–metal batteries. Nanoscale, 2020, 12, 15528-15559.	2.8	31
27	A non-nucleophilic gel polymer magnesium electrolyte compatible with sulfur cathode. Nano Research, 2020, 13, 2749-2754.	5.8	20
28	Multi‧tep Phase Transitions of Mn <sub>3</sub> O <sub>4</sub> During Galvanostatic Lithiation: An In Situ Transmission Electron Microscopic Investigation. Small, 2020, 16, e1906499.	5.2	4
29	Multi-ion Modulated Single-Step Synthesis of a Nanocarbon Embedded with a Defect-Rich Nanoparticle Catalyst for a High Loading Sulfur Cathode. ACS Applied Materials & Interfaces, 2020, 12, 12727-12735.	4.0	27
30	Solubility-Dependent Protective Effects of Binary Alloys for Lithium Anode. ACS Applied Energy Materials, 2020, 3, 2278-2284.	2.5	16
31	Single atomic cobalt catalyst significantly accelerates lithium ion diffusion in high mass loading Li2S cathode. Energy Storage Materials, 2020, 28, 375-382.	9.5	92
32	Singleâ€Atomic Catalysts Embedded on Nanocarbon Supports for High Energy Density Lithium–Sulfur Batteries. ChemSusChem, 2020, 13, 3404-3411.	3.6	41
33	High-performance Oxygen Evolution Catalyst Enabled by Interfacial Effect between CeO <sub>2</sub> and FeNi Metal-organic Framework. Acta Chimica Sinica, 2020, 78, 355.	0.5	6
34	Graphene edge-enhanced anchoring of the well-exposed cobalt clusters <i>via</i> strong chemical bonding for accelerating the oxygen reduction reaction. Sustainable Energy and Fuels, 2019, 3, 2859-2866.	2.5	6
35	Hierarchical Sulfur-Doped Graphene Foam Embedded with Sn Nanoparticles for Superior Lithium Storage in LiFSI-Based Electrolyte. ACS Applied Materials & Interfaces, 2019, 11, 30500-30507.	4.0	27
36	Coupling Niobia Nanorods with a Multicomponent Carbon Network for High Power Lithium-Ion Batteries. ACS Applied Materials & Interfaces, 2019, 11, 44196-44203.	4.0	14

#	Article	IF	CITATIONS
37	Commercial-Level Energy Storage via Free-Standing Stacking Electrodes. Matter, 2019, 1, 1694-1709.	5.0	19
38	Freestanding Carbon Nanotube Film for Flexible Straplike Lithium/Sulfur Batteries. Chemistry - A European Journal, 2019, 25, 3775-3780.	1.7	23
39	A highly integrated All-manganese battery with oxide nanoparticles supported on the cathode and anode by super-aligned carbon nanotubes. Journal of Materials Chemistry A, 2019, 7, 4494-4504.	5.2	21
40	All-solid-state sponge-like squeezable zinc-air battery. Energy Storage Materials, 2019, 23, 375-382.	9.5	47
41	High areal capacity flexible sulfur cathode based on multi-functionalized super-aligned carbon nanotubes. Nano Research, 2019, 12, 1105-1113.	5.8	28
42	<i>In Situ</i> X-ray Absorption Spectroscopic Investigation of the Capacity Degradation Mechanism in Mg/S Batteries. Nano Letters, 2019, 19, 2928-2934.	4.5	63
43	Single-atom catalyst boosts electrochemical conversion reactions in batteries. Energy Storage Materials, 2019, 18, 246-252.	9.5	203
44	Improving a Mg/S Battery with YCl <sub>3</sub> Additive and Magnesium Polysulfide. Advanced Science, 2019, 6, 1800981.	5.6	50
45	Infiltrating lithium into carbon cloth decorated with zinc oxide arrays for dendrite-free lithium metal anode. Nano Research, 2019, 12, 525-529.	5.8	79
46	Synergistic effects of CuO and Au nanodomains on Cu2O cubes for improving photocatalytic activity and stability. Chinese Journal of Catalysis, 2019, 40, 105-113.	6.9	30
47	Stretchable fiber-shaped lithium metal anode. Energy Storage Materials, 2019, 22, 179-184.	9.5	65
48	Free-Standing Black Phosphorus Thin Films for Flexible Quasi-Solid-State Micro-Supercapacitors with High Volumetric Power and Energy Density. ACS Applied Materials & Interfaces, 2019, 11, 5938-5946.	4.0	31
49	Allâ€Solidâ€State Fiber Supercapacitors with Ultrahigh Volumetric Energy Density and Outstanding Flexibility. Advanced Energy Materials, 2019, 9, 1802753.	10.2	197
50	Simultaneously Regulating Lithium Ion Flux and Surface Activity for Dendrite-Free Lithium Metal Anodes. ACS Applied Materials & Interfaces, 2019, 11, 5159-5167.	4.0	33
51	Lithium nitrate: A double-edged sword in the rechargeable lithium-sulfur cell. Energy Storage Materials, 2019, 16, 498-504.	9.5	39
52	A non-nucleophilic mono-Mg2+ electrolyte for rechargeable Mg/S battery. Energy Storage Materials, 2018, 14, 253-257.	9.5	40
53	In Situ Electrochemically Derived Amorphousâ€Li <sub>2</sub> S for High Performance Li <sub>2</sub> S/Graphite Full Cell. Small, 2018, 14, e1703871.	5.2	29
54	Tuning active sites on cobalt/nitrogen doped graphene for electrocatalytic hydrogen and oxygen evolution. Electrochimica Acta, 2018, 265, 497-506.	2.6	56

#	Article	IF	CITATIONS
55	Achieving commercial-level mass loading in ternary-doped holey graphene hydrogel electrodes for ultrahigh energy density supercapacitors. Nano Energy, 2018, 46, 266-276.	8.2	135
56	Ultrafast Allâ€Solidâ€State Coaxial Asymmetric Fiber Supercapacitors with a High Volumetric Energy Density. Advanced Energy Materials, 2018, 8, 1702946.	10.2	86
57	Free-Standing, Binder-Free Titania/Super-Aligned Carbon Nanotube Anodes for Flexible and Fast-Charging Li-Ion Batteries. ACS Sustainable Chemistry and Engineering, 2018, 6, 3426-3433.	3.2	34
58	Interfacial Energy-Level Alignment for High-Performance All-Inorganic Perovskite CsPbBr <sub>3</sub> Quantum Dot-Based Inverted Light-Emitting Diodes. ACS Applied Materials & Interfaces, 2018, 10, 13236-13243.	4.0	44
59	Converting detrimental HF in electrolytes into a highly fluorinated interphase on cathodes. Journal of Materials Chemistry A, 2018, 6, 17642-17652.	5.2	116
60	Reducing lithium deposition overpotential with silver nanocrystals anchored on graphene aerogel. Nanoscale, 2018, 10, 16562-16567.	2.8	44
61	(Invited) Light Absorption Enhancement Using Graphene Quantum Dots in Dye-Sensitized Solar Cells and Photoelectrochemical Water Splitting. ECS Meeting Abstracts, 2018, , .	0.0	0
62	Graphene quantum dot antennas for high efficiency Förster resonance energy transfer based dye-sensitized solar cells. Journal of Power Sources, 2017, 343, 39-46.	4.0	35
63	Liquidâ€Phase Electrochemical Scanning Electron Microscopy for In Situ Investigation of Lithium Dendrite Growth and Dissolution. Advanced Materials, 2017, 29, 1606187.	11.1	128
64	Photocatalytic performance enhancement of CuO/Cu2O heterostructures for photodegradation of organic dyes: Effects of CuO morphology. Applied Catalysis B: Environmental, 2017, 211, 199-204.	10.8	136
65	High Electroactive Material Loading on a Carbon Nanotube@3D Graphene Aerogel for Highâ€Performance Flexible Allâ€Solidâ€State Asymmetric Supercapacitors. Advanced Functional Materials, 2017, 27, 1701122.	7.8	138
66	Synergistic promotion of photoelectrochemical water splitting efficiency of TiO 2 nanorods using metal-semiconducting nanoparticles. Applied Surface Science, 2017, 420, 631-637.	3.1	25
67	Reduced graphene oxide coated porous carbon–sulfur nanofiber as a flexible paper electrode for lithium–sulfur batteries. Nanoscale, 2017, 9, 9129-9138.	2.8	53
68	Wrapping Aligned Carbon Nanotube Composite Sheets around Vanadium Nitride Nanowire Arrays for Asymmetric Coaxial Fiber-Shaped Supercapacitors with Ultrahigh Energy Density. Nano Letters, 2017, 17, 2719-2726.	4.5	281
69	Improved cycling stability of the capping agent-free nanocrystalline FeS2 cathode via an upper cut-off voltage control. Journal of Materials Science, 2017, 52, 2442-2451.	1.7	20
70	Temperature-Dependent Electron–Electron Interaction in Graphene on SrTiO <sub>3</sub> . Nano Letters, 2017, 17, 5914-5918.	4.5	17
71	Folded-up thin carbon nanosheets grown on Cu <sub>2</sub> O cubes for improving photocatalytic activity. Nanoscale, 2017, 9, 12348-12352.	2.8	17
72	Robust electrical "highway―network for high mass loading sulfur cathode. Nano Energy, 2017, 40, 390-398.	8.2	68

#	Article	IF	CITATIONS
73	Fieldâ€Induced nâ€Doping of Black Phosphorus for CMOS Compatible 2D Logic Electronics with High Electron Mobility. Advanced Functional Materials, 2017, 27, 1702211.	7.8	95
74	A Conversation with Yuegang Zhang. ACS Central Science, 2017, 3, 1131-1132.	5.3	0
75	Constructing Ultrahigh-Capacity Zinc–Nickel–Cobalt Oxide@Ni(OH) <sub>2</sub> Core–Shell Nanowire Arrays for High-Performance Coaxial Fiber-Shaped Asymmetric Supercapacitors. Nano Letters, 2017, 17, 7552-7560.	4.5	231
76	Stretchable fiber-shaped asymmetric supercapacitors with ultrahigh energy density. Nano Energy, 2017, 39, 219-228.	8.2	200
77	Progress of Lithium/Sulfur Batteries Based on Chemically Modified Carbon. Wuli Huaxue Xuebao/ Acta Physico - Chimica Sinica, 2017, 33, 165-182.	2.2	15
78	Preparation of Three-dimensional Nitrogen-doped Carbon Nanoribbon and Application in Lithium/Sulfur Batteries. Acta Chimica Sinica, 2017, 75, 225.	0.5	3
79	Seleniumâ€Ðoped Black Phosphorus for Highâ€Responsivity 2D Photodetectors. Small, 2016, 12, 5000-5007.	5.2	156
80	Prelithiation of Nanostructured Sulfur Cathode by an "Onâ€Sheet―Solidâ€State Reaction. Small, 2016, 12, 4966-4972.	5.2	14
81	Simultaneous optimization of surface chemistry and pore morphology of 3D graphene-sulfur cathode via multi-ion modulation. Journal of Power Sources, 2016, 321, 193-200.	4.0	46
82	Impact of size on energy storage performance of graphene based supercapacitor electrode. Electrochimica Acta, 2016, 219, 463-469.	2.6	32
83	Controlling Electrochemical Lithiation/Delithiation Reaction Paths for Long-cycle Life Nanochain-structured FeS2 Electrodes. Electrochimica Acta, 2016, 211, 671-678.	2.6	15
84	Intrinsic factors attenuate the performance of anhydride organic cathode materials of lithium battery. Journal of Electroanalytical Chemistry, 2016, 773, 22-26.	1.9	12
85	Carbon Nitride Supramolecular Hybrid Material Enabled High-Efficiency Photocatalytic Water Treatments. Nano Letters, 2016, 16, 6568-6575.	4.5	108
86	Efficient solar-driven water splitting by nanocone BiVO <sub>4</sub> -perovskite tandem cells. Science Advances, 2016, 2, e1501764.	4.7	351
87	Highly defective graphite for scalable synthesis of nitrogen doped holey graphene with high volumetric capacitance. Journal of Power Sources, 2016, 334, 104-111.	4.0	30
88	Ultra-endurance flexible all-solid-state asymmetric supercapacitors based on three-dimensionally coated MnOx nanosheets on nanoporous current collectors. Nano Energy, 2016, 26, 610-619.	8.2	103
89	Synthesis, Crystal Structure, and Electrochemical Properties of a Simple Magnesium Electrolyte for Magnesium/Sulfur Batteries. Angewandte Chemie, 2016, 128, 6516-6520.	1.6	38
90	Synthesis, Crystal Structure, and Electrochemical Properties of a Simple Magnesium Electrolyte for Magnesium/Sulfur Batteries. Angewandte Chemie - International Edition, 2016, 55, 6406-6410.	7.2	106

#	ARTICLE	IF	CITATIONS
91	Layered Lithium-Rich Oxide Nanoparticles Doped with Spinel Phase: Acidic Sucrose-Assistant Synthesis and Excellent Performance as Cathode of Lithium Ion Battery. ACS Applied Materials & Interfaces, 2016, 8, 4575-4584.	4.0	119
92	Chemical routes toward long-lasting lithium/sulfur cells. Nano Research, 2016, 9, 94-116.	5.8	112
93	A dual-spatially-confined reservoir by packing micropores within dense graphene for long-life lithium/sulfur batteries. Nanoscale, 2016, 8, 2395-2402.	2.8	43
94	In-situ TEM Study of the Liquid-Phase Reaction of Ag Nanowires with a Sulfur Solution. Acta Chimica Sinica, 2016, 74, 980.	0.5	0
95	Effects of cell construction parameters on the performance of lithium/sulfur cells. AICHE Journal, 2015, 61, 2749-2756.	1.8	6
96	Highly Nitridated Graphene–Li <sub>2</sub> S Cathodes with Stable Modulated Cycles. Advanced Energy Materials, 2015, 5, 1501369.	10.2	97
97	Fabrication of Nb2O5 Nanosheets for High-rate Lithium Ion Storage Applications. Scientific Reports, 2015, 5, 8326.	1.6	123
98	Vertically Aligned Carbon Nanotubes on Carbon Nanofibers: A Hierarchical Three-Dimensional Carbon Nanostructure for High-Energy Flexible Supercapacitors. Chemistry of Materials, 2015, 27, 1194-1200.	3.2	113
99	Dense integration of graphene and sulfur through the soft approach for compact lithium/sulfur battery cathode. Nano Energy, 2015, 12, 468-475.	8.2	142
100	Synthesis of three-dimensional hyperbranched TiO <sub>2</sub> nanowire arrays with significantly enhanced photoelectrochemical hydrogen production. Journal of Materials Chemistry A, 2015, 3, 4004-4009.	5.2	43
101	A high energy density Li <sub>2</sub> S@C nanocomposite cathode with a nitrogen-doped carbon nanotube top current collector. Journal of Materials Chemistry A, 2015, 3, 18913-18919.	5.2	55
102	A Graphene-like Oxygenated Carbon Nitride Material for Improved Cycle-Life Lithium/Sulfur Batteries. Nano Letters, 2015, 15, 5137-5142.	4.5	358
103	Fabrication of mesoporous Li <sub>2</sub> S–C nanofibers for high performance Li/Li <sub>2</sub> S cell cathodes. Nanoscale, 2015, 7, 9472-9476.	2.8	43
104	All-Solid-State High-Energy Asymmetric Supercapacitors Enabled by Three-Dimensional Mixed-Valent MnO <sub><i>x</i></sub> Nanospike and Graphene Electrodes. ACS Applied Materials & Interfaces, 2015, 7, 22172-22180.	4.0	59
105	Surface-enhanced Raman scattering from AgNP–graphene–AgNP sandwiched nanostructures. Nanoscale, 2015, 7, 17529-17537.	2.8	37
106	Tuning plasmonic and chemical enhancement for SERS detection on graphene-based Au hybrids. Nanoscale, 2015, 7, 20188-20196.	2.8	85
107	Synthesis of V <sub>2</sub> O <sub>5</sub> hierarchical structures for long cycle-life lithium-ion storage. Journal of Materials Chemistry A, 2015, 3, 1103-1109.	5.2	43

Large-scale fabrication of graphene-based electronic and MEMS devices. , 2014, , .

#	Article	IF	CITATIONS
109	Three-dimensional metal/oxide nanocone arrays for high-performance electrochemical pseudocapacitors. Nanoscale, 2014, 6, 3626-3631.	2.8	57
110	Polarized X-ray Absorption Spectroscopy Observation of Electronic and Structural Changes of Chemical Vapor Deposition Graphene in Contact with Water. Journal of Physical Chemistry C, 2014, 118, 25456-25459.	1.5	23
111	Enhanced Charge Collection for Splitting of Water Enabled by an Engineered Three-Dimensional Nanospike Array. Journal of Physical Chemistry C, 2014, 118, 22465-22472.	1.5	16
112	High-Rate, Ultralong Cycle-Life Lithium/Sulfur Batteries Enabled by Nitrogen-Doped Graphene. Nano Letters, 2014, 14, 4821-4827.	4.5	683
113	Polyaniline-modified cetyltrimethylammonium bromide-graphene oxide-sulfur nanocomposites with enhanced performance for lithium-sulfur batteries. Nano Research, 2014, 7, 1355-1363.	5.8	63
114	Distinguishing Localized Surface Plasmon Resonance and Schottky Junction of Au–Cu <sub>2</sub> O Composites by Their Molecular Spacer Dependence. ACS Applied Materials & Interfaces, 2014, 6, 10958-10962.	4.0	63
115	Efficient Photoelectrochemical Water Splitting with Ultrathin films of Hematite on Three-Dimensional Nanophotonic Structures. Nano Letters, 2014, 14, 2123-2129.	4.5	307
116	Wafer-Scale Integration of Graphene-based Electronic, Optoelectronic and Electroacoustic Devices. Scientific Reports, 2014, 4, 3598.	1.6	113
117	Variability Effects in Graphene: Challenges and Opportunities for Device Engineering and Applications. Proceedings of the IEEE, 2013, 101, 1670-1688.	16.4	29
118	A Long-Life, High-Rate Lithium/Sulfur Cell: A Multifaceted Approach to Enhancing Cell Performance. Nano Letters, 2013, 13, 5891-5899.	4.5	404
119	Supramolecular polymers with tunable topologies via hierarchical coordination-driven self-assembly and hydrogen bonding interfaces. Proceedings of the National Academy of Sciences of the United States of America, 2013, 110, 15585-15590.	3.3	221
120	Scalable and Direct Growth of Graphene Micro Ribbons on Dielectric Substrates. Scientific Reports, 2013, 3, 1348.	1.6	36
121	Laser directed lithography of asymmetric graphene ribbons on a polydimethylsiloxane trench structure. Physical Chemistry Chemical Physics, 2013, 15, 6825.	1.3	7
122	In-Situ XAS Investigation of the Effect of Electrochemical Reactions on the Structure of Graphene in Aqueous Electrolytes. Journal of the Electrochemical Society, 2013, 160, C445-C450.	1.3	23
123	Lithium/sulfur batteries with high specific energy: old challenges and new opportunities. Nanoscale, 2013, 5, 2186.	2.8	480
124	Nanowire-based resistive switching memories: devices, operation and scaling. Journal Physics D: Applied Physics, 2013, 46, 074006.	1.3	50
125	Monitoring Oxygen Movement by Raman Spectroscopy of Resistive Random Access Memory with a Graphene-Inserted Electrode. Nano Letters, 2013, 13, 651-657.	4.5	121
126	A Long-Life, High-Rate Lithium/Sulfur Cell. ECS Meeting Abstracts, 2013, , .	0.0	0

#	Article	IF	CITATIONS
127	Electrode/oxide interface engineering by inserting single-layer graphene: Application for HfO <inf>x</inf> -based resistive random access memory. , 2012, , .		12
128	Nanostructured Li <sub>2</sub> S–C Composites as Cathode Material for High-Energy Lithium/Sulfur Batteries. Nano Letters, 2012, 12, 6474-6479.	4.5	286
129	Graphene/Si multilayer structure anodes for advanced half and full lithium-ion cells. Nano Energy, 2012, 1, 164-171.	8.2	151
130	Fermi velocity engineering in graphene by substrate modification. Scientific Reports, 2012, 2, .	1.6	344
131	Direct Growth of Graphene Nanoribbons for Large-Scale Device Fabrication. Nano Letters, 2012, 12, 6175-6179.	4.5	42
132	Hard HfB <sub>2</sub> tip-coatings for ultrahigh density probe-based storage. Applied Physics Letters, 2012, 101, 091909.	1.5	6
133	SnS2 nanoparticle loaded graphene nanocomposites for superior energy storage. Physical Chemistry Chemical Physics, 2012, 14, 6981.	1.3	79
134	Electronic structure and chemical bonding of a graphene oxide–sulfur nanocomposite for use in superior performance lithium–sulfur cells. Physical Chemistry Chemical Physics, 2012, 14, 13670.	1.3	305
135	Electronic structure study of ordering and interfacial interaction in graphene/Cu composites. Carbon, 2012, 50, 5316-5322.	5.4	32
136	Graphene Oxide-Sulfur Nanocomposites for Advanced Lithium/Sulfur Cell Cathodes. ECS Meeting Abstracts, 2012, , .	0.0	0
137	Electronic transport properties of zigzag carbon- and boron-nitride-nanotube heterostructures. Solid State Communications, 2012, 152, 1061-1066.	0.9	27
138	Edge Effect on Resistance Scaling Rules in Graphene Nanostructures. Nano Letters, 2011, 11, 1082-1086.	4.5	37
139	Linewidth roughness in nanowire-mask-based graphene nanoribbons. Applied Physics Letters, 2011, 98, 243118.	1.5	13
140	Multilayer nanoassembly of Sn-nanopillar arrays sandwiched between graphene layers for high-capacity lithium storage. Energy and Environmental Science, 2011, 4, 3611.	15.6	218
141	Graphene Oxide as a Sulfur Immobilizer in High Performance Lithium/Sulfur Cells. Journal of the American Chemical Society, 2011, 133, 18522-18525.	6.6	1,415
142	Fe3O4 nanoparticle-integrated graphene sheets for high-performance half and full lithium ion cells. Physical Chemistry Chemical Physics, 2011, 13, 7170.	1.3	238
143	Porous carbon nanofiber–sulfur composite electrodes for lithium/sulfur cells. Energy and Environmental Science, 2011, 4, 5053.	15.6	562
144	Resistiveâ€ <b>6</b> witching Crossbar Memory Based on Ni–NiO Core–Shell Nanowires. Small, 2011, 7, 2899-2905.	5.2	71

#	Article	IF	CITATIONS
145	Fully inverted single-digit nanometer domains in ferroelectric films. Applied Physics Letters, 2010, 96, .	1.5	17
146	Enhanced Conductance Fluctuation by Quantum Confinement Effect in Graphene Nanoribbons. Nano Letters, 2010, 10, 4590-4594.	4.5	27
147	An Ultraclean Tip-Wear Reduction Scheme for Ultrahigh Density Scanning Probe-Based Data Storage. ACS Nano, 2010, 4, 5713-5720.	7.3	21
148	Low-noise submicron channel graphene nanoribbons. Applied Physics Letters, 2010, 97, 073107.	1.5	19
149	Direct Chemical Vapor Deposition of Graphene on Dielectric Surfaces. Nano Letters, 2010, 10, 1542-1548.	4.5	439
150	Metal-catalyzed crystallization of amorphous carbon to graphene. Applied Physics Letters, 2010, 96, .	1.5	234
151	Effect of Spatial Charge Inhomogeneity on 1/ <i>f</i> Noise Behavior in Graphene. Nano Letters, 2010, 10, 3312-3317.	4.5	83
152	Electrostatic Force Assisted Exfoliation of Prepatterned Few-Layer Graphenes into Device Sites. Nano Letters, 2009, 9, 467-472.	4.5	112
153	Carbon nanofiber supercapacitors with large areal capacitances. Applied Physics Letters, 2009, 95, .	1.5	123
154	Gate-Variable Optical Transitions in Graphene. Science, 2008, 320, 206-209.	6.0	1,433
155	Nanopencil as a wear-tolerant probe for ultrahigh density data storage. Applied Physics Letters, 2008, 93, .	1.5	22
156	SWCNT growth on Al/Fe/Mo investigated byin situmass spectroscopy. Nanotechnology, 2007, 18, 185709.	1.3	13
157	Analytical model for subthreshold conduction and threshold switching in chalcogenide-based memory devices. Journal of Applied Physics, 2007, 102, .	1.1	507
158	Evidence for trap-limited transport in the subthreshold conduction regime of chalcogenide glasses. Applied Physics Letters, 2007, 90, 192102.	1.5	153
159	Measurement of Scattering Rate and Minimum Conductivity in Graphene. Physical Review Letters, 2007, 99, 246803.	2.9	905
160	Room-Temperature Quantum Hall Effect in Graphene. Science, 2007, 315, 1379-1379.	6.0	2,662
161	High sensitivity and nonlinearity of carbon nanotube charge-based sensors. Journal of Applied Physics, 2006, 99, 084301.	1.1	12
162	Controlled Precipitation of Solubilized Carbon Nanotubes by Delamination of DNA. Journal of Physical Chemistry B, 2006, 110, 54-57.	1.2	51

#	Article	IF	CITATIONS
163	CARBON NANOTUBE BASED NONVOLATILE MEMORY DEVICES. International Journal of High Speed Electronics and Systems, 2006, 16, 959-975.	0.3	5
164	Carbon nanotube-based nonvolatile memory with charge storage in metal nanocrystals. Applied Physics Letters, 2005, 87, 043108.	1.5	43
165	In situ Raman and fluorescence monitoring of optically trapped single-walled carbon nanotubes. , 2004, 5593, 73.		1
166	Electric Field Effect in Atomically Thin Carbon Films. Science, 2004, 306, 666-669.	6.0	56,177
167	Optical Trapping of Single-Walled Carbon Nanotubes. Nano Letters, 2004, 4, 1415-1419.	4.5	121
168	Composite Nanowires. , 2003, , 257-268.		0
169	X-ray photoelectron microscopy of the C 1s core level of free-standing single-wall carbon nanotube bundles. Applied Physics Letters, 2002, 80, 2165-2167.	1.5	38
170	Abnormal anti-Stokes Raman scattering of carbon nanotubes. Physical Review B, 2002, 66, .	1.1	22
171	Imaging as-grown single-walled carbon nanotubes originated from isolated catalytic nanoparticles. Applied Physics A: Materials Science and Processing, 2002, 74, 325-328.	1.1	132
172	Growth of Single-Walled Carbon Nanotubes from Discrete Catalytic Nanoparticles of Various Sizes. Journal of Physical Chemistry B, 2001, 105, 11424-11431.	1.2	648
173	Noncovalent Sidewall Functionalization of Single-Walled Carbon Nanotubes for Protein Immobilization. Journal of the American Chemical Society, 2001, 123, 3838-3839.	6.6	2,472
174	Electric-field-directed growth of aligned single-walled carbon nanotubes. Applied Physics Letters, 2001, 79, 3155-3157.	1.5	568
175	Molecular photodesorption from single-walled carbon nanotubes. Applied Physics Letters, 2001, 79, 2258-2260.	1.5	357
176	Structure modification of single-wall carbon nanotubes. Carbon, 2000, 38, 2055-2059.	5.4	121
177	Metal coating on suspended carbon nanotubes and its implication to metal–tube interaction. Chemical Physics Letters, 2000, 331, 35-41.	1.2	576
178	Large scale synthesis of single-wall carbon nanotubes by arc-discharge method. Journal of Physics and Chemistry of Solids, 2000, 61, 1031-1036.	1.9	147
179	Microstructural evolution of single-walled carbon nanotubes under electron irradiation. Philosophical Magazine Letters, 2000, 80, 427-433.	0.5	8
180	Coiled structure of eccentric coaxial nanocable made of amorphous boron and silicon oxide. Applied Physics Letters, 2000, 76, 1564-1566.	1.5	25

#	Article	IF	CITATIONS
181	Controllable method for fabricating single-wall carbon nanotube tips. Applied Physics Letters, 2000, 77, 966.	1.5	5
182	Temperature dependence of the Raman spectra of single-wall carbon nanotubes. Applied Physics Letters, 2000, 76, 2053-2055.	1.5	154
183	Formation of metal nanowires on suspended single-walled carbon nanotubes. Applied Physics Letters, 2000, 77, 3015-3017.	1.5	363
184	Single-wall carbon nanotube colloids in polar solvents. Chemical Communications, 2000, , 461-462.	2.2	32
185	Elastic Response of Carbon Nanotube Bundles to Visible Light. Physical Review Letters, 1999, 82, 3472-3475.	2.9	157
186	Formation of single-wall carbon nanotubes by laser ablation of fullerenes at low temperature. Applied Physics Letters, 1999, 75, 3087-3089.	1.5	101
187	Mass-production of single-wall carbon nanotubes by arc discharge method11This work was supported by the National Natural Science Foundation of China, No. 29671030 Carbon, 1999, 37, 1449-1453.	5.4	207
188	Dependence of Elastic Properties on Morphology in Single-Wall Carbon Nanotubes. Advanced Materials, 1999, 11, 931-934.	11.1	14
189	Heterostructures of Single-Walled Carbon Nanotubes and Carbide Nanorods. Science, 1999, 285, 1719-1722.	6.0	385
190	Production of Single-Wall Carbon Nanotubes at High Pressure. Journal of Physical Chemistry B, 1999, 103, 8698-8701.	1.2	38
191	Defects in arc-discharge-produced single-walled carbon nanotubes. Philosophical Magazine Letters, 1999, 79, 473-479.	0.5	48
192	Structure modelling of Â3 and Â9 coincident boundaries in CVD diamond thin films. Journal of Electron Microscopy, 1999, 48, 245-251.	0.9	15
193	Coaxial Nanocable: Silicon Carbide and Silicon Oxide Sheathed with Boron Nitride and Carbon. , 1998, 281, 973-975.		491
194	Single-wall carbon nanotubes synthesized by laser ablation in a nitrogen atmosphere. Applied Physics Letters, 1998, 73, 3827-3829.	1.5	124
195	Microscopic structure of as-grown single-wall carbon nanotubes by laser ablation. Philosophical Magazine Letters, 1998, 78, 139-144.	0.5	19
196	Atomie and Electron Structure of Diamond Grain boundaries in a Polycrystalline Film. Materials Research Society Symposia Proceedings, 1997, 472, 93.	0.1	0
197	Heterogeneous growth of Bî—,Cî—,N nanotubes by laser ablation. Chemical Physics Letters, 1997, 279, 264-269.	1.2	209
198	Transmission Electron Microscopic Observation of Grain Boundaries in CVD Diamond Thin Films. Journal of Electron Microscopy, 1996, 45, 436-441.	0.9	9

#	Article	IF	CITATIONS
199	Application of Spatially Resolved Eels on Atomic Structure Determination of Diamond Grain Boundary. Materials Research Society Symposia Proceedings, 1996, 466, 273.	0.1	2
200	Atomic and Electronic Structures of Grain Boundary in Chemical Vapor Deposited Diamond Thin Film. Materials Research Society Symposia Proceedings, 1995, 416, 355.	0.1	3
201	In—situ fabrication of YBCO/YSZ/Si thin films by laser ablation. Physica C: Superconductivity and Its Applications, 1991, 185-189, 1997-1998.	0.6	3
202	Ultrahigh Density Probe-based Storage Using Ferroelectric Thin Films. , 0, , .		3